

1 Article

2

Towards Sensor Reliability Using Internet-of-Things

3

LiDAR Data in a Cyber-Physical System

4 **Fernando Castaño^{1,*}, Alberto Villalonga¹, Rodolfo E. Haber¹, Joanna Kossakowska² and**
5 **Stanisław Strzelczak²**6 ¹ Centre for Automation and Robotics (CSIC –UPM), Spanish National Research Council, Arganda del Rey,
7 Madrid, 28500, Spain; rodolfo.haber@car.upm-csic.es8 ² Faculty of Production Engineering, Warsaw University of Technology, Warsaw, Poland;
9 s.strzelczak@wip.pw.edu.pl

10 * Correspondence: fernando.castano@car.upm-csic.es; Tel.: +34-918-70-50 (F.C.)

11

12 **Abstract:** Currently, the most important challenge in any assessment of state-of-the-art sensor
13 technology and its reliability is to achieve road traffic safety targets. The research reported in this
14 paper is focused on the design of a procedure for evaluating the reliability of Internet-of-Things
15 (IoT) sensors and the use of a Cyber-Physical System (CPS) for the implementation of that evaluation
16 procedure to gauge reliability. An important requirement for the generation of real critical situations
17 under safety conditions is the capability of managing a co-simulation environment, in which both
18 real and virtual data sensory information can be processed. An IoT case study that consists of a
19 LiDAR-based collaborative map is then proposed, in which both real and virtual computing nodes
20 with their corresponding sensors exchange information. Specifically, the sensor chosen for this
21 study is a Ibeo Lux 4-layer LiDAR sensor with IoT added capabilities. Implementation is through
22 an artificial-intelligence-based modeling library for sensor data-prediction error, at a local level, and
23 a self-learning-based decision-making model supported on a Q-learning method, at a global level.
24 Its aim is to determine the best model behavior and to trigger the updating procedure, if required.
25 Finally, an experimental evaluation of this framework is also performed using simulated and real
26 data.27 **Keywords:** Cyber-Physical Systems; reliability assessment; Internet-of-Things; LiDAR sensor;
28 driving assistance; obstacle recognition; reinforcement learning; Artificial Intelligence-based
29 modelling.

30

31

1. Introduction

32 Nowadays, knowledge of the most appropriate sensor operating conditions and fault detection
33 systems are among the cornerstones of scientific and technical studies for automated systems [1].
34 These are based upon on-line monitoring processes and additional comprehensive interpretation of
35 sensor data, by assessing sensor reliability. Sensors are driving the rapid growth of Cyber-Physical
36 Systems (CPSs) and the Internet of Things (IoT). Both paradigms are behind the next generation of
37 sensor networks and unpredictable future applications, meaning that sensor reliability has become
38 one of the most important and desirable performance indicators in the design, implementation, and
39 deployment of future sensor networks [2].40 An important reliability-related issue to be detected in autonomous systems is the failure of one
41 network element, in order to self-correct problems such as lost data packages, and data collision,
42 among others [3]. One possible solution is to build real-time prediction models that maximize
43 robustness and lifetime [4]. There are, in fact, several methods for the evaluation of sensor reliability.

44 Each component that constitutes reliability or that might affect it can be assessed individually and as

45 a whole, through a total error band figure. There are important features to be considered such as
46 sensitivity, range, precision, resolution, accuracy, offset, linearity, dynamic linearity, hysteresis and
47 response time. Evaluating sensor reliability includes probabilistic and statistical data that increase
48 estimation reliability [5]. Evidence theory can be used, such as the Dempster-Shafer theory of belief
49 functions. Quantifying reliability implies predictions concerning sensor lifetime and failure
50 probability. Reliability can therefore be based on both statistical and Artificial Intelligence (AI)
51 models. Suitable probability functions must be defined, which will be used to calculate the future
52 behavior of devices, based either on carefully controlled laboratory experiments or on thorough
53 failure analysis while in use. A typical product will be liable to various failure modes that change
54 over time in a characteristic manner, so that the probability functions are themselves time dependent.
55

56 The most widely used techniques for modelling predictions concerning product lifetime and
57 failure probability are probabilistic methods. Probabilistic methods for uncertain reasoning represent
58 another group of techniques. Probability theory predicts events from a state of partial knowledge,
59 while Fuzzy-Logic models are applied to situations with intrinsic vagueness and uncertainty.

60 However, the prediction techniques are hardly limited to those mentioned above. Several
61 clustering techniques such as nearest neighbor methods have been explored, in order to enable self-
62 detection and self-correction capabilities [6]. Other capabilities to be considered from the perspective
63 of reliability are self-adaptation and self-organization by embedding artificial neural networks
64 (ANNs) in CPSs [7]. Efficient performance of multiple sensors and their online monitoring and self-
65 correction procedures, through the application of machine learning (ML) such as Support Vector
66 Machines (SVM) and ANNs, are very important for the reduction of maintenance costs, risk
67 minimization associated with uncalibrated and faulty sensors, increased instrument reliability and,
68 consequently, extended equipment life [8, 9].

69 With the aim of guaranteeing certain safety and security conditions in some critical applications,
70 the verification of sensory data and subsequent data evaluation are described in this paper through
71 the simulation of virtual and real scenarios, as well as frameworks that properly combine both
72 scenarios.

73 A reliability assessment procedure is therefore described in this paper that is applicable to data
74 captured by IoT LiDAR sensors in automotive applications: LiDAR self-testing methodology. The
75 reliability analysis is based on the paradigm of cyber-physical systems (CPS) by distributing nodes
76 locally and globally, as will be explained later on. Each computing node has data-processing methods
77 and machine-learning models for reliability prediction. In addition, a run-time self-learning and
78 decision-making model runs within a global node, in order to determine the best model and the
79 model updating mechanism on request.

80 The paper will be organized into five sections. Following this introduction, the second section will
81 present a state-of-art review of the CPS-based reliability concept for sensor system reliability using
82 AI methods. Subsequently, the specifications and the requirements obtained from the review of CPS
83 reliability frameworks will be summarized in section 3. A particular implementation of a CPS-based
84 co-simulation framework will also be proposed in this section. In addition, a case study for the
85 evaluation of an IoT sensor network using a CPS-based co-simulation framework approach will be
86 described in section 4. In that section, the experimental results and a discussion relating to a
87 comparative study will also be addressed. Finally, the conclusions and future research steps will be
88 presented in section 5.

88 **2. CPS-based reliability approach**

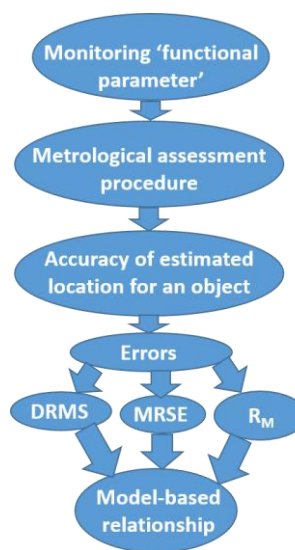
89 The truly challenging aspects of sensor network reliability and its evaluation have yet to prompt
90 an exhaustive exploration and evaluation of sensory data under critical conditions. A gap that is
91 addressed in this study through sensors incorporated in a CPS.

92
93

94 *2.1. Sensor reliability assessment*

95 One approach to sensor reliability in automotive applications is to design a model-based
 96 relationship between 'model parameters'. Those parameters can be derived from process monitors
 97 while 'functional parameters' refer to both the sensor characteristics and sensor lifetime, as well as
 98 cost aspects due to process yields (see Figure 1).

99 With the aim of increasing the reliability of data collected by LIDAR, metrological assessment
 100 procedures must also be applied. Linear interpolation of measurements from three detectors
 101 arranged in series is a time-saving procedure for processing and reducing LIDAR data [10].
 102



103

104 **Figure 1.** Procedure for sensor reliability assessment using model-based relationship between sensor
 105 data and key performance indices.

106 All the major sources of potential error that could influence point positioning accuracy have to
 107 be considered in the analytical derivations, in order to determine the reliability of achievable point
 108 positioning accuracy of LiDAR systems. Csanyi, May and Toth provided some of the random errors
 109 that will be considered [11]. They also provided some formulas for point positioning accuracy that
 110 were derived from the LiDAR equation, via rigorous error propagation:
 111

$$r_M = r_{M,INS} + R_{INS}^M (R_L^{INS} \cdot r_L + b_{INS}) \quad (1)$$

112

113 where, r_M represents the 3D coordinates of an object point in the mapping frame; $r_{M,INS}$ represents
 114 time dependent 3D INS coordinates in the mapping frame, provided by GPS/INS; R_{INS}^M is the time
 115 dependent rotation matrix between the INS body and the mapping frame; R_L^{INS} is the boresight
 116 matrix between the laser frame and the INS body frame; r_L represents the 3D object coordinates in
 117 the laser frame; and, b_{INS} is the boresight offset vector.

118 In addition, the calculation of the accuracy of the estimated location for an object using the
 119 LiDAR sensor can be performed by other key performance indices. For example, the use of the
 120 Distance Root Mean Squared (DRMS) measure for the data that are tracked on the x-y plane (2D) and
 121 the Mean Radial Spherical Error (MRSE) measure for the data that are tracked in the x-y-z space (3D)
 122 were reported in [12, 13]. Using derivable error formulas, any given random error and scan angle in
 123 the LiDAR range can be modelled and simulated. By doing so, the factors affecting LiDAR system
 124 accuracy can be analyzed [14].

125 2.2. Statistical and Artificial Intelligence-based methods

126 Bayesian and Hidden Markov models are the most widely applied for reliability assessment
 127 under fuzzy environments [15, 16]. A Bayesian network is a directed acyclic graph consisting of a set
 128 of nodes, representing random variables and a set of directed edges, representing their conditional

129 dependencies. The dependencies in a Bayesian network can be adaptively determined from a dataset
130 through a learning process. The objective of this training is to induce the network with the best
131 description of the probability distribution over the dataset and can be categorized as an unsupervised
132 learning method, because the attribute values are not supplied in the dataset [17].

133 In addition to those probabilistic methods, new tools are reported in the literature, highlighting
134 the use of Artificial Intelligence (AI) techniques and in particular, Machine Learning (ML), to solve
135 complex situations [18]. AI techniques also provide cognitive abilities, so that performance may be
136 improved by increasing network life-time and reliability [19]. Some of those techniques are ANN and
137 fuzzy inference system [20, 21]. Zhang et al. proposed a soft-computing system based on Genetic
138 Algorithm-Support Vector Regression (GA-SVR), in order to facilitate the reliability and survivability
139 of the Structural Health Monitoring (SHM) system faced, for example, with an invalid fiber link in
140 the sensor network [22].

141 3. CPS-based co-simulation framework

142 Some factors that can affect CPS reliability are component failure, environmental effects, task
143 changes, and network update. A strategy for testing the reliability of CPSs and for their evaluation is
144 proposed in [23] by analyzing both the internal and the external factors that influence their reliability.
145 One solution could be to evaluate each element that constitutes the system: testing hardware,
146 software, and architecture, as well as performance reliability including service reliability, cyber
147 security reliability, resilience & elasticity reliability, and vulnerability reliability.

148 Behavioral simulations of CPS and IoT assume importance as a method to analyze reliability,
149 because the mathematical modeling of those factors is so difficult [24]. Those simulations are based
150 on addressing four main topics: node localization, energy management, network multi-objective
151 optimization, and self-capabilities approach [25, 26].

152 While the reliability evaluation of physical systems is well-understood and has been extensively
153 studied, the reliability evaluation of a CPS is of greater complexity, because software systems will not
154 degrade and follow a well-defined failure model in the same way as physical systems. An evaluation
155 framework is therefore necessary, in order to assess the CPSs. A framework for CPS reliability
156 analysis that includes reliability-based runtime reconfiguration is proposed in [27]. This framework
157 is codified in a domain-specific modelling language that provides details on operational constraints
158 and dependences.

159 However, domain-specific modelling-based analysis is, in many cases, unable to compute
160 reliability functions efficiently (e.g. in terms of failure distributions) for complex systems. To do so, a
161 frequency-domain reliability analysis framework of transportation CPSs was described in [28]. The
162 advantage of that method is its capability to capture higher-order moments of the system
163 characteristics, its scalability for the analysis of the reliability of complex systems, and efficient
164 calculations.

165 In addition, it is important to consider the evaluation of other aspects of the CPS, such as safety
166 and particularly security, different aspects of which have been focused upon over the past few years.
167 Therefore, the design of the CPS framework must address those aspects at three levels: security
168 objectives, security approaches and security in specific applications [29]. However, not only must the
169 cyber part be secured, but also the physical part of possible threats. A multi-cyber (computational
170 unit) framework was compared with traditional models to improve the availability of the CPS based
171 on the Markov model. It was efficiently evaluated, in terms of availability, downtime, downtime
172 costs, and the reliability of the CPS framework [30].

173 Finally, another work considered an Internet-based computing platform in the form of a global
174 computing node. In [31], a new cloud security management framework was introduced, based on
175 improving collaboration between cloud providers, service providers, and service consumers for the
176 management of cloud platform security and the hosting services. In addition, although in some
177 applications this will not be possible, it is important to consider the possibility of introducing the
178 human factor in the reliability analysis procedure. A human-interactive Hardware-In-the-Loop

179 Simulation (HILS) framework for CPS was developed in [32] to support reliability and reusability in
 180 a fully distributed operating environment.

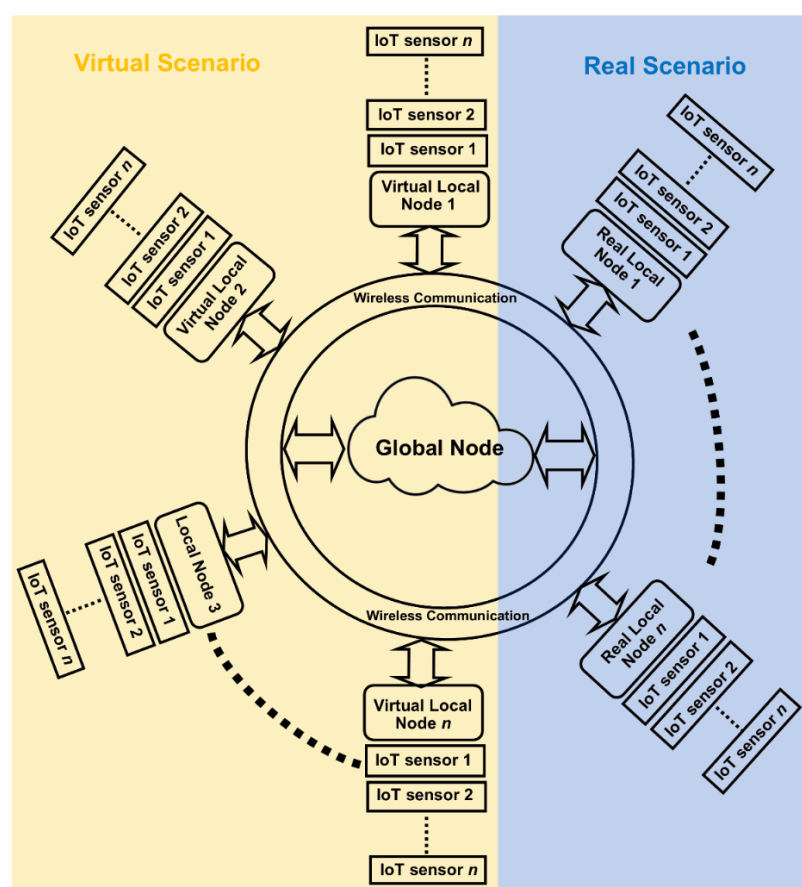
181 *3.1. CPS-based co-simulation framework proposed*

182 Based on the above contributions and considering the initial list of requirements from the
 183 previous section for the deployment of an IoT sensor network, a CPS-based co-simulation framework
 184 is proposed where an IoT sensor network will supply physical data and (local and global) computing
 185 nodes for processing the sensory data.

186 *3.1.1. Conceptual Scheme*

187 In addition, the IoT sensor network has a global or main node composed of a knowledge
 188 database, a Q-learning method for decision-making and an AI-based model library. During the
 189 simulation and the real running, a decision-making module will decide which specific model is the
 190 best in the current instant, taking into account the data received by all nodes that make up the
 191 network.

192 The functionalities are distributed in different nodes, both virtual and real, according to their
 193 functions. The distributed virtual or real nodes manage the capture of sensory data and run the error
 194 prediction calculation with the required accuracy, while the global or main node incorporates the
 195 runtime model that is generated, the library, and the knowledge database (see Figure 2).
 196



197

198 **Figure 2.** General scheme of the CPS-based co-simulation framework with virtual and real computing
 199 nodes and IoT sensor network.

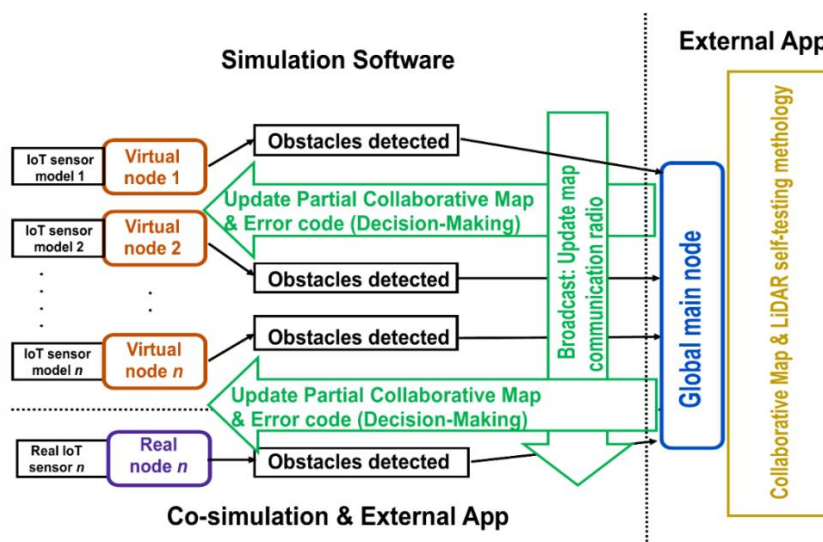
200 The IoT sensors should be able to establish reliable and accurate wireless communications,
 201 ensuring that all the intrinsic challenges in an IoT network and in the different CPSs can be solved. It
 202 is achieved through the implementation of the architecture that is represented in Figure 2: a network

203 of n nodes, each node having n IoT sensors. In addition, the computing nodes must communicate
204 with each other and with their corresponding global node.

205 **3.1.2. Procedure description**

206 The framework is designed with the condition that both the real and the virtual (local)
207 computing nodes must operate in parallel with the global computing node [33]. Data exchange
208 between the different nodes takes place in two different ways. On the one hand, data exchange
209 between local nodes is produced in both the virtual (3D model simulation tool) and the real scenario.
210 On the other hand, there is the data exchange between different local nodes and the global node using
211 the 802.11p wireless communication protocol.

212 There is therefore interaction between the software for both the simulated and the real
213 environments, and external applications that are running in the main node. Figure 3 shows the
214 schematic diagram of the exchange of information or messages within the co-simulation framework.
215



216

217 **Figure 3.** Conceptual flowchart showing the operation of a reliability co-simulation framework with
218 CPS computing nodes and IoT sensors.

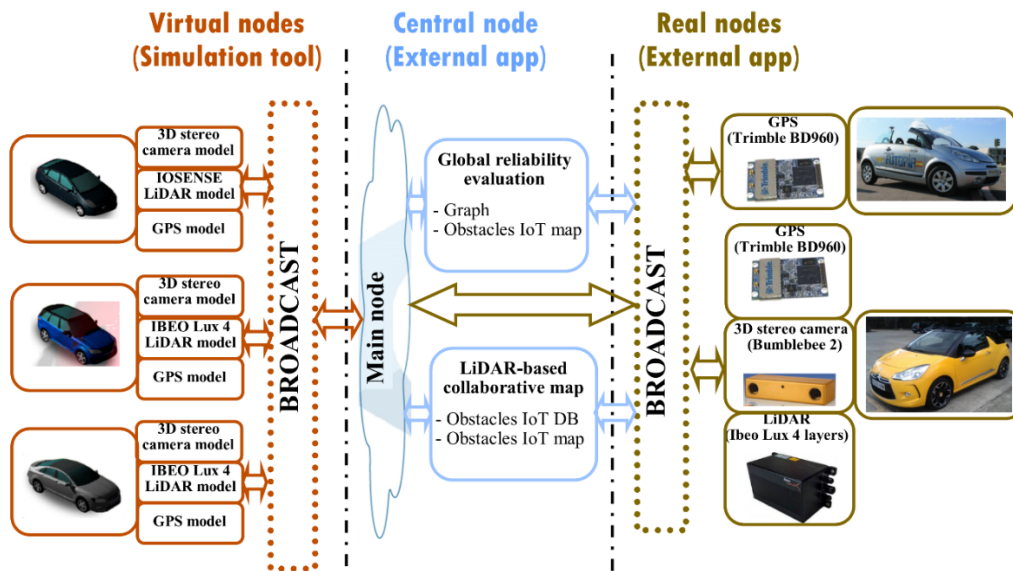
219 In the particular implementation that is described more accurately in the following section, there
220 is a wireless exchange of messages between different nodes using the 802.11p communication
221 protocol in the following way. First, the local nodes with their IoT sensors detect different objects and
222 their respective properties. Secondly, this information is shared on the network through a broadcast
223 process.

224 **4. IoT LiDAR-based collaborative mapping – A case study**

225 The IoT sensor network chosen to evaluate the CPS-based co-simulation framework is composed
226 of virtual and real LiDAR sensors [34]. An Ibeo Lux LiDAR 4-layer sensor was used with the
227 following specifications: horizontal field of 120 deg, horizontal step of 0.125 deg., vertical field of 3.2
228 deg., vertical step of 0.8 deg., range of 200 m, and an update frequency of 12.5 Hz. As previously
229 mentioned, the sensor network to be evaluated is composed of IoT sensors. The sensor network
230 therefore has IoT capabilities connected to its computing nodes. These nodes are on-board computers
231 integrated in an autonomous vehicle with a wireless communication interface between them.

232 The particular implementation of the CPS-based co-simulation framework, the LiDAR-based
233 collaborative map, is based on a co-simulation framework between two different software systems,
234 both for the simulated part, designed in [35]. However, the contribution of this study is to include the
235 real part in the co-simulation framework. This framework consists mainly of a computer-aided
236 system to enable efficient interaction between the virtual scenario with virtual nodes setting in the
237 Webots automobile simulation tool 8.6 [36] and an external application development for the

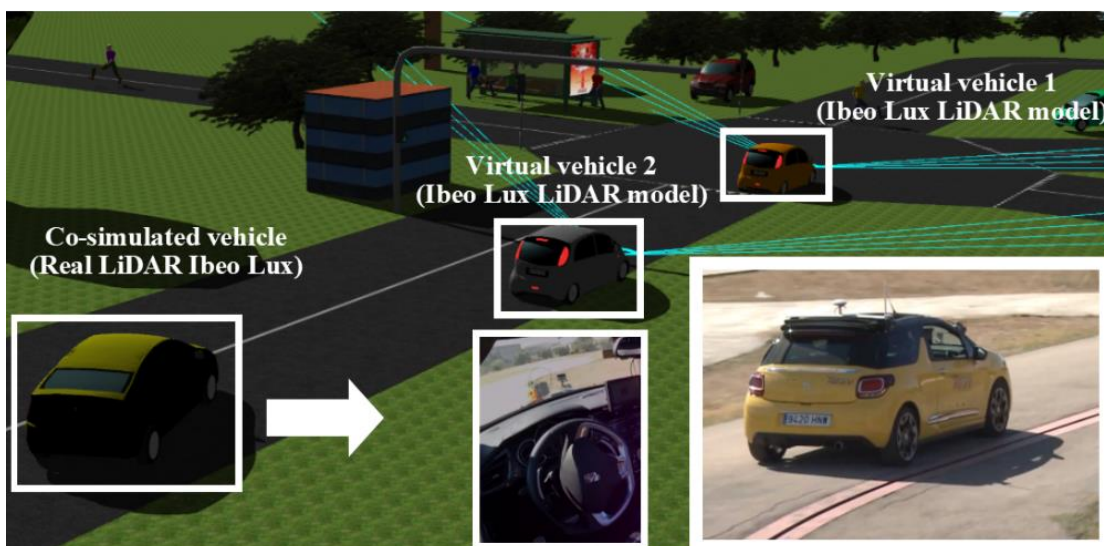
238 computing nodes in the real scenario. The scenario in this particular case, in which the vehicles are
 239 represented as nodes, is as follows. A real vehicle (in a real scenario) and three virtual vehicles in the
 240 simulated scenario are detecting obstacles. Both kinds of vehicles share the position, object type and
 241 size of the obstacles (e.g., pedestrian, trees on the road and another vehicle). This is possible thanks
 242 to the IoT LiDAR network using an IoT obstacle detection application (see section 4.1), created in run
 243 time. Figure 4 shows the detailed diagram of the implementation of the LiDAR-based collaborative
 244 map using the CPS-based framework approach.
 245



246

247 **Figure 4.** Detailed diagram of the implementation of the LiDAR-based collaborative map approached
 248 through a CPS-based co-simulation framework.

249 As previously mentioned above, the exchange of information packets between the local nodes
 250 with the main or global node is possible; thanks to the use of a communication protocol using a UDP
 251 (User Datagram Protocol) as the transport layer and a Wi-Fi 802.11p as the physical layer. The
 252 visualization of the co-simulated vehicle (real node) in the 3D virtual scenario in the Webots
 253 simulation tool is also possible. An example of the execution of the co-simulation architecture can be
 254 seen in Figure 5.
 255



256

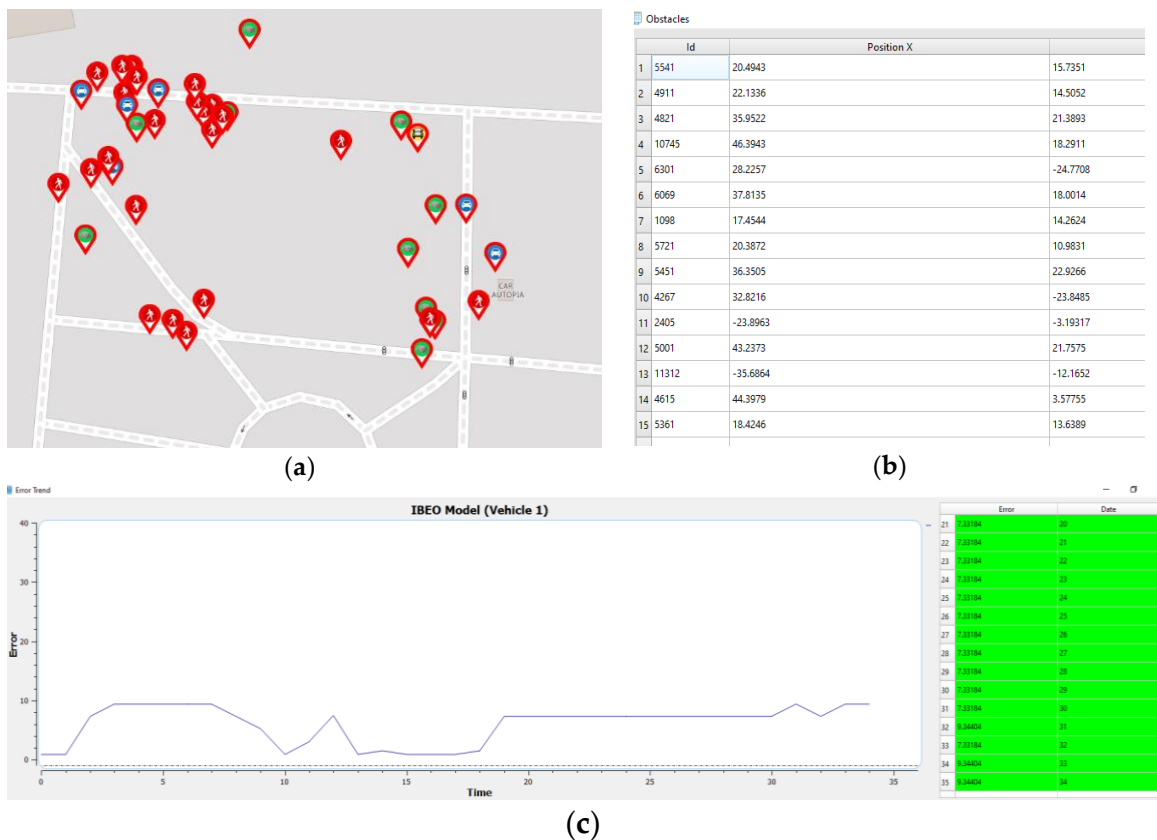
257 **Figure 5.** Data interchange between LiDAR sensors in (virtual and real) driving assistance scenarios
 258 in Webots for automobiles.

259 In addition, another application implemented in the IoT LiDAR-based collaborative map is the
 260 LiDAR self-testing methodology incorporated in each local computing node (autonomous vehicle),
 261 in order to evaluate the reliability of each IoT sensor in the network (section 4.2).

262 *4.1 Obstacle detection in the IoT application*

263 This framework is implemented in an external application; a development in Qt 5.10, that
 264 consists of an illustrated map updated in run time (see Figure 6 (a)) and a database with the
 265 information on both the virtual and the real objects that are detected (see Figure (b)). The information
 266 contains the position, object type, and size of the obstacles, to improve on the security/safety of the
 267 object detection process with a single sensor.

268



269 **Figure 6.** (a) Collaborative mapping; (b) obstacles detected database; (c) LiDAR data for run-time
 270 accuracy error detection.

271 Figure 6 depicts the visual interface of the framework that has been developed. Specifically, the
 272 collaborative map is globally updated in the main computing node. A partial area of this updated
 273 map can also be sent at the request of a local node. A set of computational procedures is in charge of
 274 adapting and transferring sensory information from Webots, virtual nodes with the Ibeo Lux sensor
 275 model, and the real node, real vehicles with the real Ibeo Lux sensor; and vice versa.

276 *4.2. LiDAR self-testing application*

277 The external application also includes a LiDAR data self-testing methodology using the AI-
 278 based error-prediction models. Figure 6 (c) shows the graphical interface that represents the
 279 estimated error with regard to time on the left-hand side. However, on the right-hand side the
 280 admissible error threshold is observed, which if exceeded, must be requested to make decisions over
 281 the best performance of each model at any given time. Specifically, the results are focused on showing
 282 the improved performance of the IoT sensor network composed of each CPS element with each

283 LiDAR sensor plus added IoT capabilities. To do so, a reliability prediction model dedicated to
284 obtaining the accuracy error in obstacle detection is incorporated in each computing node.

285 **4.2.1. Reliability prediction models**

286 A reliability model was generated for each IoT LiDAR sensor, both virtual and real, that
287 predicted the accuracy error for obstacle detection. The steps to follow for the determination of those
288 models were extracted from the methodology described in [37, 38], with a set of different training
289 data. In this study, a model-based procedure was used with a point-cloud clustering technique, in
290 this case Density-Based Spatial Clustering of Applications with Noise (DBSCAN) [39]. In addition,
291 an error-based prediction model library was described, highlighting AI-based model techniques,
292 such as, Multilayer Perceptron Neural Network (MLP), k-Nearest Neighbors (*k*-NN), and Linear
293 Regression (LR). A difference in the particular implementation described in this paper is that, while
294 *k*-NN, MLP and LR were maintained, SVM was added as a new technique to the AI-based library
295 [40-42].

296 **4.2.2. Model parametrization and validation**

297 With the aim of determining which model training strategy based on AI provides the best
298 reliability prediction model, an experimental validation was performed. The training dataset was
299 composed of 998 scenes for the model training and 250 scenes for the model validation. All of them
300 were obtained from a simulation procedure. The data input consisted of geospatial statistics [13, 43]
301 which were extracted from the point cloud supplied by the LiDAR sensor, so that the models could
302 generate the figures of merit in terms of accuracy error: DRMS and MRSE.

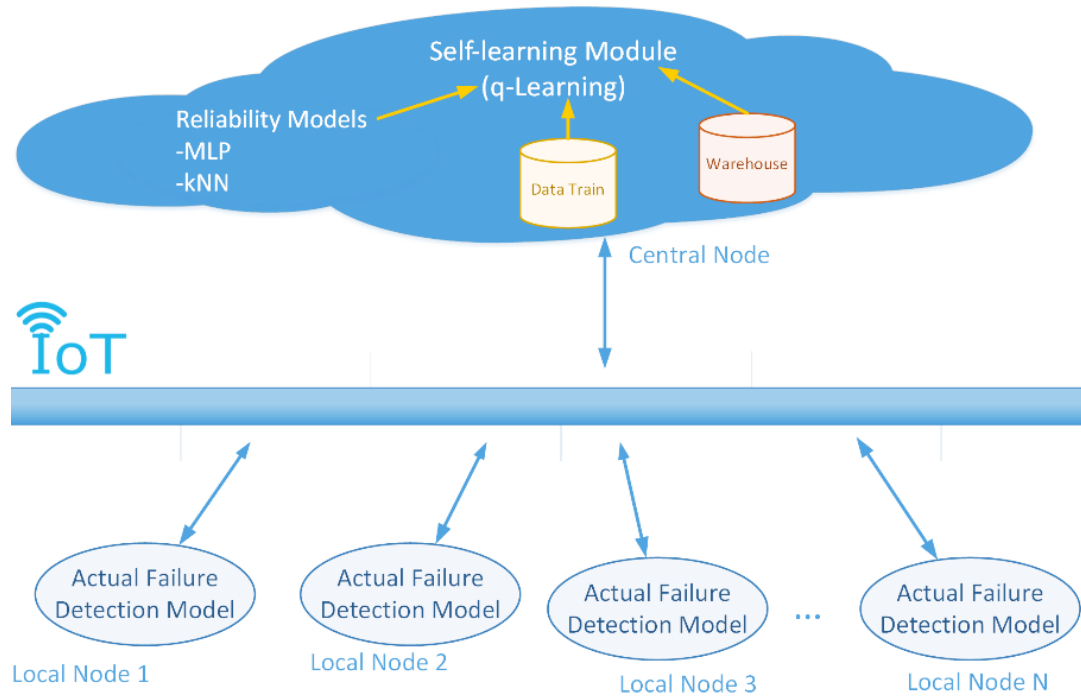
303 The four AI-based strategies that were considered are as follows. First, a multilayer perceptron
304 neural network with backpropagation (MLP) with two hidden layers, each with five neurons and
305 sigmoid activation functions, and an output layer with a lineal activation function, two neurons, and
306 5000 epochs. The initial value of the learning rate (μ) was 10-3 with a decrease factor ratio of 10-1, an
307 increase factor ratio of 10, and a maximum μ value of 1010. The minimum performance gradient was
308 10-7. The training process stop criteria were as follows: the maximum number of epochs (repetitions);
309 goal performance minimization; the performance gradient below a minimum gradient; or, a μ value
310 in excess of the maximum value. The second modeling technique was *k*-nearest neighbors (*k*-NN),
311 with *k* = 5 and using Euclidean distance as the distance function. The third was a lineal regression
312 that was also obtained by minimizing the sum of squared differences between the predicted and the
313 observed values. Finally, a support vector machine model was fitted by means of data
314 standardization and the radial basis function kernel.

315 **4.2.3. Self-learning-based decision-making. Q-learning algorithm**

316 The global or main computing node executes several parallel procedures in a specific self-
317 learning module that uses a Q-learning algorithm. On the one hand, a dataset for training by default
318 is present in the global node. On the other hand, a knowledge database (warehouse) is also included,
319 which can be updated in run time with the data provided by each local node. It sets up the self-
320 learning strategy that is run, in order to analyze the best model behavior, when new traffic situations
321 are generated providing new point clouds (environment information).

322 The local node, also in parallel, simulates the reliability model and when an error is admissible
323 the threshold will exceed 20% in one the figures of merits (DRMS or MRSE), which will mean that
324 the current model is failing. A request is therefore made to the global module to establish whether
325 there is a model that is working better. The decision to select the best prediction model included in
326 the library is taken by the self-learning decision-making at each instant, according to the
327 generalization capability and the accuracy of the model. The particular performance metrics for each
328 are R^2 and RAE, respectively. In summary, based on this continuous information flow and the
329 previous prediction results (knowledge database), when a request from one of the local nodes is

330 received and a new best model behavior is detected, the current error prediction model is then
 331 commuted, between MLP and k-NN, and vice versa.
 332



333
 334 **Figure 9.** Flow diagram between the global node (self-learning module), IoT network, and local
 335 nodes (actual failure detection model).

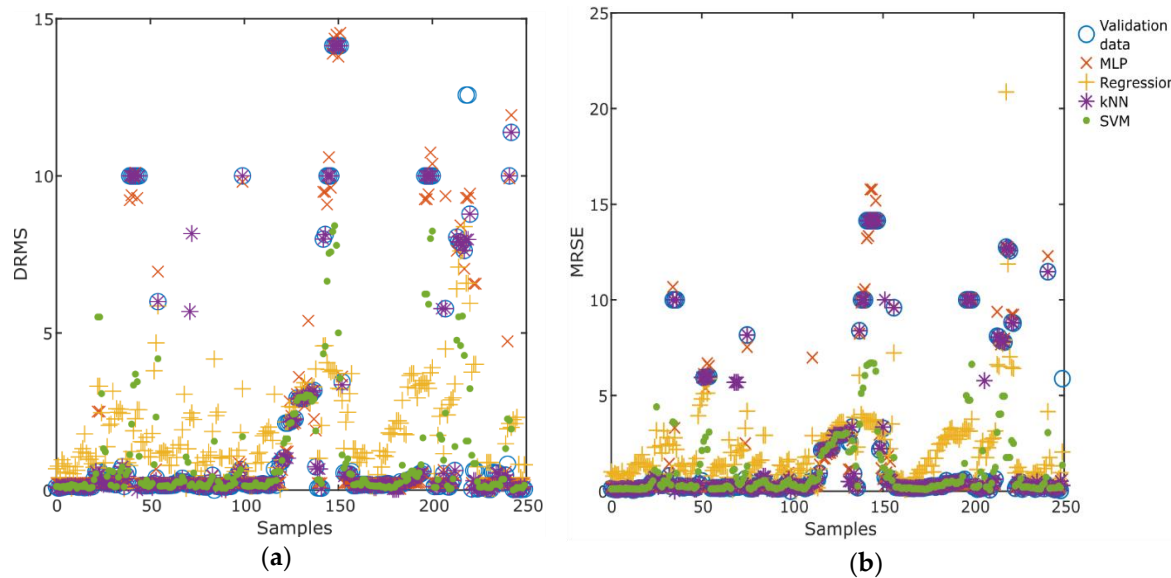
336 5. Experimental results

337 5.1. Reliability model-based validation

338 **Table 1.** Key performance indices based on plane (DMRS) & space (MRSE) figure of merits.

Model	MAE		RMSE		RAE		RRSE		R ²	
	DMRS	MRSE	DMRS	MRSE	DMRS	MRSE	DMRS	MRSE	DMRS	MRSE
MLP	0.0046	0.0035	1.275	1.270	0.187	0.188	0.395	0.392	0.933	0.933
kNN	0.002	0.0002	1.014	1.010	0.114	0.114	0.371	0.365	0.963	0.961
LR	0.6781	0.6530	2.305	2.285	0.701	0.695	0.782	0.788	0.434	0.435
SVM	0.4735	0.4740	2.072	2.065	0.442	0.447	0.773	0.773	0.692	0.684

339
 340 Table 1 shows the evaluation results obtained during the initial validation of each reliability
 341 model. Five error-based performance indices and two classification criteria were considered in the
 342 validation process: Mean Absolute Error (MAE); Root Mean Squared Error (RMSE); Relative
 343 Absolute Error (RAE); Root Relative Squared Error (RRSE); and, the coefficient of determination (R²).
 344 Only, the models generated with k-NN and MLP returned R² results higher than 90%.
 345



346 **Figure 7.** Behavior representation of LiDAR error on the plane for each model with regard to the
 347 validation data.

348 Figure 7 illustrates the behavior representation of the LiDAR error on the plane (DRMS) for each
 349 model (MLP, LN, KNN and SVM) with regard to the validation data. The AI-based modeling
 350 techniques that showed the best performing were MLP and KNN, according to the comparative study
 351 of the four modelling strategies, with a percentage improved performance comparable to the other
 352 two models of around 30%. Those model types will be chosen for the validation of the decision-
 353 making module.

354 *5.1. Self-learning for decision-making evaluation*

355 Finally, a simulation in order to determine the quality of the Q-learning method in the automatic
 356 selection of the best prediction model was performed. The reward function is chosen for setting the
 357 best possible Q-value in 100 different scenes. Therefore, the function to update the Q-values is [44]:
 358

$$Q_{t+1}(s_t, a_t) = Q_t(s_t, a_t) + \alpha_t(s_t, a_t)(R_{t+1} + \gamma \max_{a \in A} Q_t(s_{t+1}, a) - Q_t(s_t, a_t)) \quad (2)$$

359 where, s_t is the state in time t ; a_t is the action taken in time t ; $R_{(t+1)}$ is the reward received after
 360 performing action a_t ; α_t is the learning rate; and, γ is the discount factor which trades off the
 361 importance of sooner-versus-later rewards. Table 2 lists the error reward matrix based on knowledge
 362 of the behavior of those prediction models.

363
 364 **Table 2.** Q-learning reward matrix for error admissible threshold.

R ²	RAE				
	0 - 10%	10 - 20%	20 - 40%	40 - 70%	> 70%
90 - 100%	1	0.9	0.8	0.5	0.2
80 - 90%	0.85	0.8	0.65	0.4	0.15
70 - 80%	0.7	0.6	0.5	0.3	0.1
30 - 60%	0.5	0.4	0.3	0.2	0.05
0 - 30%	0.3	0.2	0.15	0.1	0.01

365
 366
 367 The decision-making was based on two of the main performance indexes of model quality. First,
 368 the coefficient of determination (R^2) was taken into consideration, as it provides a measure of the

369 generalization capacity of the model. The Relative Absolute Error (RAE), which is a measure of model
 370 accuracy, was the second parameter.

371 Figure 9 shows the Q-learning classification error matrix. As previously shown, the best model
 372 had a RAE between 0 and 20% and a R^2 above 80% in 61% of the scenarios. The system was able to
 373 guarantee models with a greater capability of generalization in 71% of the scenarios, based on a
 374 coefficient of determination that was over 80%. In total, reliability can be predicted with an RAE of
 375 less than 40% and an R^2 of over 70% in 90% of the scenarios, which demonstrates the quality of the
 376 models. The models presented a low generalization, with a coefficient of determination of less than
 377 70% in only 9% of the scenarios and a RAE greater than 40% in only 1%. Therefore, the Q-learning
 378 method that evaluates reliability on the basis of the prediction error model at each instant worked
 379 appropriately when determining the best model that represented the LiDAR performance to a high
 380 degree of accuracy and that guaranteed the required levels of safety and reliability for automotive
 381 applications.

382

		RAE				
		0-10%	10-20%	20-40%	40-70%	70-100%
R^2	90-100%	9%	7%			
	80-90%	12%	33%	10%		
	70-80%		19%		1%	
	60-70%		7%	2%		
	0-30%					

383

384 **Figure 9.** Q-learning classification error matrix.

385 **5. Conclusions**

386 A method and an accompanying procedure have been presented in this paper for evaluating the
 387 reliability of IoT sensors in a CPS. A co-simulation platform has been designed for that purpose where
 388 virtual and real sensors can interact during run time through different simulations under appropriate
 389 safety conditions. The co-simulation framework was composed of distributed computing nodes
 390 within an IoT network, at both global and local levels.

391 A case study that consists of a LiDAR-based collaborative map has been proposed, in order to
 392 validate the CPS-based co-simulation framework. Real and virtual computing nodes with the
 393 corresponding sensors shared the position, object type, and size of the obstacles, to improve the
 394 security and safety of the autonomous driving when detecting objects with this framework in run
 395 time. The assessment of the proposed method was divided into two parallel procedures. First, at local
 396 level, each reliability model evaluated the condition of the IoT LiDAR sensor. Secondly, at a global
 397 level, a self-learning strategy for decision-making determined the most appropriate behavior of
 398 models in the reliability model library, also in run time. The Q-learning method was selected for this
 399 unsupervised self-learning strategy.

400 The comparative study of four strategies (MLP, SVM, k-NN and linear regression) in the
 401 reliability modelling library was then performed. In summary, the MLP and the k-NN methods
 402 outperformed the other two strategies considered in this study. Based on the previous results, a final
 403 experimental evaluation was presented, in order to determine the quality of the Q-learning method
 404 for automatically selecting the best reliability model. A Q-learning method evaluated the reliability
 405 models, in order to perform the analysis, in a simulation study with 100 different scenarios. Based on

406 this procedure and the prediction results of the Q-learning method, when a request from one of the
407 local nodes is received, a new model behavior is detected, and the current error prediction model is
408 then commuted. Overall, all the reliability models performed very well, according to their
409 generalization capability.

410 Therefore, the proposed CPS-based co-simulation framework has served to assess the
411 performance of the IoT LiDAR network very accurately, guaranteeing safety and reliability in this
412 autonomous driving case study. These promising results pave the way for future work that will
413 validate the proposed method under real autonomous driving conditions.

414 **Author Contributions:** R.E.H., J.K. and S.S reviewed all technical and scientific aspects of the article. A.V. and
415 F.C. was in charge of the implementation of software application, the library models and the reinforcement
416 learning algorithm. F.C. and A.V. designed and implemented the scenario, the external application and the
417 LiDAR self-testing procedure, and drafted the paper.

418 **Acknowledgments:** This work was partially supported by the project Power2Power: Providing next-generation
419 silicon-based power solutions in transport and machinery for significant decarbonisation in the next decade,
420 funded by the Electronic Component Systems for European Leadership (ECSEL-JU) Joint Undertaking and the
421 Ministry of Science, Innovation and Universities (MICINN), under grant agreement No 826417. In addition, this
422 work was also funded by the Spanish Ministry of Science, Innovation and Universities through the project
423 COGDRIVE (DPI2017-86915-C3-1-R). Preparation of this publication was also partially co-financed by the Polish
424 National Agency for Academic Exchange (NAWA) through the project: "Industry 4.0 in Production and
425 Aeronautical Engineering (IPAE)".

426 **Conflicts of Interest:** The authors declare no conflict of interest.

427

428 **References**

429 1. Beruvides, G.; Quiza, R.; Del Toro, R.; Haber, R. E., Sensing systems and signal analysis to monitor
430 tool wear in microdrilling operations on a sintered tungsten-copper composite material. *Sensors and
431 Actuators, A: Physical* **2013**, *199*, 165-175.

432 2. Kabashkin, I.; Kundler, J., Reliability of Sensor Nodes in Wireless Sensor Networks of Cyber Physical
433 Systems. *Procedia Computer Science* **2017**, *104*, 380-384.

434 3. Godoy, J.; Pérez, J.; Onieva, E.; Villagrá, J.; Milanés, V.; Haber, R., A driverless vehicle demonstration
435 on motorways and in urban environments. *Transport* **2015**, *30*, (3), 253-263.

436 4. Hao, X.; Wang, L.; Yao, N.; Geng, D.; Chen, B., Topology control game algorithm based on Markov
437 lifetime prediction model for wireless sensor network. *Ad Hoc Networks* **2018**, *78*, 13-23.

438 5. Guo, H.; Shi, W.; Deng, Y., Evaluating Sensor Reliability in Classification Problems Based on Evidence
439 Theory. *IEEE Transactions on Systems, Man, and Cybernetics, Part B (Cybernetics)* **2006**, *36*, (5), 970-981.

440 6. Zhang, H.; Liu, J.; Pang, A.-C., A Bayesian network model for data losses and faults in medical body
441 sensor networks. *Computer Networks* **2018**, *143*, 166-175.

442 7. Serpen, G.; Li, J.; Liu, L., AI-WSN: Adaptive and Intelligent Wireless Sensor Network. *Procedia Computer
443 Science* **2013**, *20*, 406-413.

444 8. Nsabagwa, M.; Mugume, I.; Kasumba, R.; Muhamuza, J.; Byarugaba, S.; Tumwesigye, E.; Otim, J. S. In
445 *Condition Monitoring and Reporting Framework for Wireless Sensor Network-based Automatic Weather
446 Stations*, 2018 IST-Africa Week Conference (IST-Africa), 9-11 May 2018, 2018; pp Page 1 of 8-Page
447 8 of 8.

448 9. Chuan, Y.; Chen, L., The Application of Support Vector Machine in the Hysteresis Modeling of Silicon
449 Pressure Sensor. *IEEE Sensors Journal* **2011**, *11*, (9), 2022-2026.

450 10. Rodrigues, C. E. D.; Da Silva, R. P. M.; Nunes, R. A., Metrological assessment of LIDAR signals in water.
451 *Measurement: Journal of the International Measurement Confederation* **2011**, *44*, (1), 11-17.

452 11. Yang, X.; Quan, Z.; Dan, J., The effect of INS and GPS random error on positioning accuracy of airborne
453 LIDAR system. *Journal of Computational Information Systems* **2011**, *7*, (11), 3795-3802.

454 12. Castaño, F.; Beruvides, G.; Villalonga, A.; Haber, R. E., Self-tuning method for increased obstacle
455 detection reliability based on internet of things LiDAR sensor models. *Sensors (Switzerland)* **2018**, *18*, (5).

456 13. Maalek, R.; Sadeghpour, F., Accuracy assessment of ultra-wide band technology in locating dynamic
457 resources in indoor scenarios. *Automation in Construction* **2016**, *63*, 12-26.

458 14. Dan, J.; Yang, X., Modeling of range and scan angle random errors from airborne LIDAR. *Journal of
459 Computational Information Systems* **2013**, *9*, (7), 2747-2753.

460 15. Wu, H. C., Bayesian system reliability assessment under fuzzy environments. *Reliability Engineering and
461 System Safety* **2004**, *83*, (3), 277-286.

462 16. Wu, H. C., Fuzzy Bayesian system reliability assessment based on exponential distribution. *Applied
463 Mathematical Modelling* **2006**, *30*, (6), 509-530.

464 17. Du, K. L.; Swamy, M. N. s., Probabilistic and Bayesian Networks. In 2014; pp 563-619.

465 18. La Fe-Perdomo, I.; Beruvides, G.; Quiza, R.; Haber, R.; Rivas, M., Automatic Selection of Optimal
466 Parameters Based on Simple Soft-Computing Methods: A Case Study of Micromilling Processes. *IEEE
467 Transactions on Industrial Informatics* **2019**, *15*, (2), 800-811.

468 19. Gheisari, S.; Meybodi, M. R., A new reasoning and learning model for Cognitive Wireless Sensor
469 Networks based on Bayesian networks and learning automata cooperation. *Computer Networks* **2017**,
470 124, 11-26.

471 20. Haber, R. E.; Alique, J. R., Nonlinear internal model control using neural networks: An application for
472 machining processes. *Neural Computing and Applications* **2004**, *13*, (1), 47-55.

473 21. Ramírez, M.; Haber, R.; Peña, V.; Rodríguez, I., Fuzzy control of a multiple hearth furnace. *Computers*
474 *in Industry* **2004**, *54*, (1), 105-113.

475 22. Zhang, X.; Liang, D.; Zeng, J.; Asundi, A., Genetic algorithm-support vector regression for high
476 reliability SHM system based on FBG sensor network. *Optics and Lasers in Engineering* **2012**, *50*, (2), 148-
477 153.

478 23. Li, Z.; Kang, R. In *Strategy for reliability testing and evaluation of cyber physical systems*, IEEE International
479 Conference on Industrial Engineering and Engineering Management, 2016; 2016; pp 1001-1006.

480 24. Vo, M.-T.; Thanh Nghi, T. T.; Tran, V.-S.; Mai, L.; Le, C.-T. In *Wireless Sensor Network for Real Time*
481 *Healthcare Monitoring: Network Design and Performance Evaluation Simulation*, Cham, 2015; Springer
482 International Publishing: Cham, 2015; pp 87-91.

483 25. Cacciagno, D.; Culmone, R.; Micheletti, M.; Mostarda, L., Energy-Efficient Clustering for Wireless
484 Sensor Devices in Internet of Things. In *Performability in Internet of Things*, Springer: 2019; pp 59-80.

485 26. Hossain, S.; Fayjie, A. R.; Doukhi, O.; Lee, D.-j. In *CAIAS Simulator: Self-driving Vehicle Simulator for AI*
486 *Research*, International Conference on Intelligent Computing & Optimization, 2018; Springer: 2018; pp
487 187-195.

488 27. Nannapaneni, S.; Mahadevan, S.; Pradhan, S.; Dubey, A. In *Towards Reliability-Based Decision Making in*
489 *Cyber-Physical Systems*, 2016 IEEE International Conference on Smart Computing, SMARTCOMP 2016,
490 2016; 2016.

491 28. Liu, X.; He, W.; Zheng, L. In *Transportation cyber-physical systems: Reliability modeling and analysis*
492 framework, National Workshop for Research on High-Confidence Transportation Cyber-Physical
493 Systems: Automotive, Aviation and Rail. November, pp 18-20.

494 29. Lu, T.; Zhao, J.; Zhao, L.; Li, Y.; Zhang, X., Towards a framework for assuring cyber physical system
495 security. *International Journal of Security and Its Applications* **2015**, *9*, (3), 25-40.

496 30. Parvin, S.; Hussain, F. K.; Hussain, O. K.; Thein, T.; Park, J. S., Multi-cyber framework for availability
497 enhancement of cyber physical systems. *Computing* **2013**, *95*, (10-11), 927-948.

498 31. Almorsy, M.; Grundy, J.; Ibrahim, A. S. In *Collaboration-based cloud computing security management*
499 framework, Proceedings - 2011 IEEE 4th International Conference on Cloud Computing, CLOUD 2011,
500 2011; 2011; pp 364-371.

501 32. Kim, M. J.; Kang, S.; Kim, W. T.; Chun, I. G. In *Human-interactive hardware-in-the-loop simulation*
502 *framework for cyber-physical systems*, 2013 2nd International Conference on Informatics and Applications,
503 ICIA 2013, 2013; 2013; pp 198-202.

504 33. Artuñedo, A.; Del Toro, R. M.; Haber, R. E., Consensus-based cooperative control based on pollution
505 sensing and traffic information for urban traffic networks. *Sensors (Switzerland)* **2017**, *17*, (5).

506 34. Godoy, J.; Haber, R.; Muñoz, J. J.; Matía, F.; García, Á., Smart sensing of pavement temperature based
507 on low-cost sensors and V2I communications. *Sensors (Switzerland)* **2018**, *18*, (7).

508 35. Castaño, F.; Beruvides, G.; Haber, R. E.; Artuñedo, A., Obstacle Recognition Based on Machine Learning
509 for On-Chip LiDAR Sensors in a Cyber-Physical System. *Sensors* **2017**, *17*, (9), 2109.

510 36. Michel, O., Cyberbotics Ltd. Webots™: professional mobile robot simulation. *International Journal of*
511 *Advanced Robotic Systems* **2004**, *1*, (1), 5.

512 37. Castaño, F.; Beruvides, G.; Villalonga, A.; Haber, R. E., Self-Tuning Method for Increased Obstacle
513 Detection Reliability Based on Internet of Things LiDAR Sensor Models. *Sensors* **2018**, *18*, (5), 1508.

514 38. Castaño, F.; Beruvides, G.; Haber, R. E.; Villalonga, A., Time-To-Failure Modelling in On-Chip LiDAR
515 Sensors for Automotive Applications. *Proceedings* **2017**, *1*, (8), 809.

516 39. Huang, F.; Zhu, Q.; Zhou, J.; Tao, J.; Zhou, X.; Jin, D.; Tan, X.; Wang, L., Research on the Parallelization
517 of the DBSCAN Clustering Algorithm for Spatial Data Mining Based on the Spark Platform. *Remote
518 Sensing* **2017**, *9*, (12), 1301.

519 40. Banerjee, T. P.; Das, S., Multi-sensor data fusion using support vector machine for motor fault detection.
520 *Information Sciences* **2012**, *217*, 96-107.

521 41. Niu, G.; Yang, B.-S.; Pecht, M., Development of an optimized condition-based maintenance system by
522 data fusion and reliability-centered maintenance. *Reliability Engineering & System Safety* **2010**, *95*, (7),
523 786-796.

524 42. Castaño, F.; Beruvides, G.; Villalonga, A.; Haber, R. E., Computational Intelligence for Simulating a
525 LiDAR Sensor. In *Sensor Systems Simulations*, Springer: 2020; pp 149-178.

526 43. Premebida, C.; Ludwig, O.; Nunes, U. In *Exploiting LiDAR-based features on pedestrian detection in urban
527 scenarios*, 2009 12th International IEEE Conference on Intelligent Transportation Systems, 4-7 Oct. 2009,
528 2009; 2009; pp 1-6.

529 44. Beruvides, G.; Juanes, C.; Castaño, F.; Haber, R. E. In *A self-learning strategy for artificial cognitive control
530 systems*, 2015 IEEE 13th International Conference on Industrial Informatics (INDIN), 22-24 July 2015,
531 2015; 2015; pp 1180-1185.

532